Peaked traveling wave solutions of the modified highly nonlinear Novikov equation

LI Hui-jun^{1,2} WEN Zhen-shu^{2,*} LI Shao-yong³

Abstract. In this paper, we focus on peaked traveling wave solutions of the modified highly nonlinear Novikov equation by dynamical systems approach. We obtain a traveling wave system which is a singular planar dynamical system with three singular straight lines, and derive all possible phase portraits under corresponding parameter conditions. Then we show the existence and dynamics of two types of peaked traveling wave solutions including peakons and periodic cusp wave solutions. The exact explicit expressions of two peakons are given. Besides, we also derive smooth solitary wave solutions, periodic wave solutions, compacton solutions, and kink-like (antikink-like) solutions. Numerical simulations are further performed to verify the correctness of the results. Most importantly, peakons and periodic cusp wave solutions are newly found for the equation, which extends the previous results.

§1 Introduction

In recent decades, many important nonlinear evolution equations have been proposed to model different nonlinear phenomena, including shallow water wave motions in fluid dynamics, ion acoustic waves in plasmas and many other engineering fields. Besides, in recent years, integrable systems also have received considerable attentions, and the inverse scattering approach and the bilinear approach have been extensively applied to study the solutions of integrable systems [1–3]. Among these equations or systems, the Camassa-Holm-type equations are of particular interest. One remarkable feature of the Camassa-Holm equation is the discovery of the so-called peakons soliton or peakons [4].

As an important Camassa-Holm-type equation, the Novikov equation

$$u_t - u_{xxt} + 4u^2 u_x = 3u u_x u_{xx} + u^2 u_{xxx}, (1)$$

 $\label{eq:Received: 2021-07-20.} Revised: 2021-12-16.$

MR Subject Classification: 34C23, 34A26, 35Q51.

Keywords: modified highly nonlinear Novikov equation, bifurcation, dynamics, peakons, periodic cusp wave solutions.

Digital Object Identifier(DOI): https://doi.org/10.1007/s11766-025-4511-7.

Supported by the National Natural Science Foundation of China (12071162), the Natural Science Foundation of Fujian Province (2021J01302), the Fundamental Research Funds for the Central Universities ($\mathbb{Z}QN-802$).

^{*}Corresponding author.

was first obtained by Novikov [5] in a symmetry classification of nonlocal partial differential equations (PDEs) with cubic nonlinearity. There has been great interest in studying the solutions of Eq.(1) and their properties. In 2008, Hong and Wang [6] proved that Eq.(1) admits N-peakon solutions. In addition, they derived a matrix Lax pair for Eq.(1) and showed that Eq.(1) possesses infinitely many conserved quantities and bi-Hamiltonian structure. Therefore Eq.(1) is integrable. Besides, there are many works [7–9] concerning the peaked solutions and their stability. More recently, by exploiting dynamical systems approach, Li [10] obtained the parametric representations of the cuspon and compactons under the condition $\varphi^2 > c$ through the traveling wave transformation $u(x,t) = \varphi(\xi), \xi = x - ct$. Further, Pan and Li [11] studied the smooth and nonsmooth solitons under the condition $\varphi^2 < c$. Zhang and Tang [12] derived the peakons and periodic cusp wave solutions of Eq.(1).

In recent years, the modified versions of Novikov equation have attracted much attention [13,14]. In this paper, we focus on the following modified highly nonlinear Novikov equation

$$u_t - u_{xxt} + 4u^4 u_x = 3u u_x u_{xx} + u^2 u_{xxx}, (2)$$

which was introduced by Zhao and Zhou [15] in 2010. It is worth mentioning that the nonlinearity of Eq.(2) is much higher than that of Eq.(1), which makes it more difficult to study the solutions of Eq.(2) and their dynamical behaviors. Zhao and Zhou [15] introduced the transformation $u(\xi) = \varphi(\xi) = \sqrt{v(\xi)}, \xi = x - ct$ and exploited symbolic computation to study its exact solutions. However, the transformation requires that $u(\xi) \geq 0$ and $v(\xi) \geq 0$ and has its limit in obtaining the solutions. Exploiting the traveling wave transformation $u(x,t) = \varphi(\xi), \xi = x - ct$ and the factorization technique, Eq.(2) can be factorized as

$$((\varphi^2 - 2) \partial_{\xi} + 3\varphi \varphi') \left(\partial_{\xi\xi} - \left(\frac{2}{3}\varphi^2 + 1\right)\right) \varphi = 0.$$
 (3)

Deng [16] obtained some special traveling wave solutions of Eq.(2) by solving the following second-order ordinary differential equation

$$\varphi'' = \varphi\left(\frac{2}{3}\varphi^2 + 1\right).$$

In fact, the solutions of Eq.(3) can be derived by solving the following coupled ordinary differential equation

$$\begin{cases}
\left(\varphi^2 - 2\right) \frac{\mathrm{d}F(\varphi(\xi))}{\mathrm{d}\xi} + 3\varphi\varphi'F(\varphi(\xi)) = 0, \\
\varphi'' - \varphi\left(\frac{2}{3}\varphi^2 + 1\right) = F(\varphi(\xi)).
\end{cases}$$
(4)

From system (4), Wen and Shi [17] showed the existence and dynamics of several types of bounded traveling wave solutions including smooth solitary wave solutions, periodic wave solutions, compacton solutions, kink-like and antikink-like solutions by dynamical systems approach. However, the peakons and periodic cusp wave solutions were not found for Eq.(2). One may wonder whether Eq.(2) has peakons and periodic cusp wave solutions, since the Novikov equation (1) and other Camassa-Holm-type equations [18,19] have peakons and periodic cusp wave solutions. Based on this motivation, in this paper, we further focus on peaked traveling wave solutions of (2) by exploiting dynamical systems approach [20–28]. For readers' convenience, here we briefly introduce the main procedure of dynamical systems approach as follows:

Step 1. Convert partial differential equation (PDE) into ordinary differential equation

(ODE) by traveling wave transformation.

- Step 2. Try to tranform the obtained ODE into planar dynamical system by some effective techniques, such as integration, multiplied by a factor [25,30] and so on, according to the special structure of ODE.
- Step 3. Based on the qualitative theories of differential equations and the bifurcation theories of dynamical systems, we can determine the bifurcation conditions and obtain the phase portraits of the above planar dynamical system.
- Step 4. Study the dynamics of traveling wave solutions through the phase portraits, and exact solutions by the first integral of planar dynamical system.

The main contributions of this paper are summarized as follows:

- (1) Showing the existence of various types of bounded traveling wave solutions including peakons, periodic cusp wave solutions, smooth solitary wave solutions, periodic wave solutions, compacton solutions, and kink-like (antikink-like) solutions under explicit parameter conditions.
- (2) Deriving the exact explicit expressions of two peakons for Eq.(2).
- (3) Observing peakons and periodic cusp wave solutions of Eq.(2) for the first time, which extends the previous works [15–17].

§2 Bifurcations of Phase Portraits

In this section, we present the bifurcations of phase portraits corresponding to (2).

To begin with, substituting $u(x,t) = \varphi(\xi)$ with $\xi = x - ct$ into (2), where c > 0 is the wave speed, it follows,

$$-c\varphi' + c\varphi''' + 4\varphi^4\varphi' = 3\varphi\varphi'\varphi'' + \varphi^2\varphi''', \tag{5}$$

where the prime stands for the derivative with respect to ξ .

Multiplying both sides of (5) by φ and integrating the equation once, we get

$$-\frac{c\varphi^2}{2} + \frac{2\varphi^6}{3} + c\varphi\varphi'' - \frac{c(\varphi')^2}{2} = \varphi^3\varphi'' - \frac{g}{6},\tag{6}$$

where q is the integral constant.

Letting $y = \varphi'$, we obtain the planar system

$$\begin{cases} \frac{d\varphi}{d\xi} = y, \\ \frac{dy}{d\xi} = \frac{4\varphi^6 - 3c\varphi^2 - 3cy^2 + g}{6\varphi(\varphi^2 - c)}, \end{cases}$$
(7)

with the following first integral

$$H_{1}(\varphi, y) = \frac{\sqrt{\varphi^{2} - c}}{\varphi} \frac{2c\varphi^{4} + 3c^{2}\varphi^{2} + 2g}{2c} - \frac{3\sqrt{\varphi^{2} - c}}{\varphi} y^{2} + \frac{3c(c - 2)}{2} \ln \left| \varphi + \sqrt{\varphi^{2} - c} \right|,$$

$$\text{for } \varphi^{2} - c > 0,$$

$$H_{2}(\varphi, y) = \frac{-\sqrt{c - \varphi^{2}}}{\varphi} \frac{2c\varphi^{4} + 3c^{2}\varphi^{2} + 2g}{2c} + \frac{3\sqrt{c - \varphi^{2}}}{\varphi} y^{2} + \frac{3c(c - 2)}{2} \arcsin \frac{\varphi}{\sqrt{c}},$$

$$\text{for } \varphi^{2} - c < 0.$$
(8)

Obviously, system (7) has three singular straight lines $\varphi = 0$, $\varphi = \sqrt{c}$ and $\varphi = -\sqrt{c}$. Transformed by $d\xi = 6\varphi(\varphi^2 - c)d\tau$, system (7) becomes a regular system

$$\begin{cases}
\frac{d\varphi}{d\tau} = 6\varphi y(\varphi^2 - c), \\
\frac{dy}{d\tau} = 4\varphi^6 - 3c\varphi^2 - 3cy^2 + g.
\end{cases}$$
(9)

Since the level curves of system (7) is the same as those of the regular system (9), we can analyze the phase portraits of system (7) from those of system (9). To study the singular points and their properties of system (9), let

$$f(\varphi) = 4\varphi^6 - 3c\varphi^2 + g. \tag{10}$$

We can obtain the graphics of the function $f(\varphi)$ in Figure 1 under corresponding parameter conditions. Note that the zeros of $f(\varphi)$ correspond to the singular points of system (9).

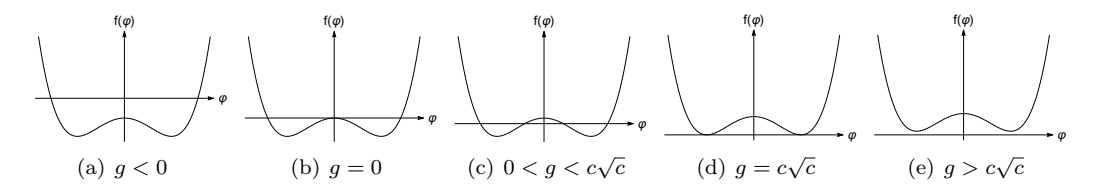


Figure 1. The graphics of the function $f(\varphi)$ under corresponding parameter conditions, (a) g < 0; (b) g = 0; (c) $0 < g < c\sqrt{c}$; (d) $g = c\sqrt{c}$; (e) $g > c\sqrt{c}$.

Let $\lambda(\varphi, y)$ be the characteristic value of the linearized system of system (9) at the singular point (φ, y) . We have

$$\lambda^2(\varphi, 0) = 6\varphi(\varphi^2 - c)f'(\varphi). \tag{11}$$

From (11), we see that the signs of φ , $\varphi^2 - c$ and $f'(\varphi)$ can determine the dynamical properties (saddle, center and degenerate singular point) of the singular point $(\varphi, 0)$ according to the theory of planar dynamical systems.

We summarize the number of singular points of system (9) and their dynamical properties under corresponding parameter conditions in Lemma 1.

Lemma 1. For system (9), we have

- (1) When $g < min\{3c^2 4c^3, 0\}$, system (9) has two singular points $(\pm \varphi_1, 0)$. Furthermore, $(\pm \varphi_1, 0)$ are saddles.
- (2) When $g = 3c^2 4c^3$ and $c > \frac{3}{4}$, system (9) has two singular points $(\pm \sqrt{c}, 0)$. Furthermore, $(\pm \sqrt{c}, 0)$ are degenerate singular points.

- (3) When $3c^2 4c^3 < g < 0$ and $c > \frac{3}{4}$, system (9) has six singular points $(\pm \varphi_1, 0)$ and $\left(\pm \sqrt{c}, \pm \sqrt{\frac{4c^3 3c^2 + g}{3c}}\right)$. Furthermore, $(\pm \varphi_1, 0)$ are centers, and $\left(\pm \sqrt{c}, \pm \sqrt{\frac{4c^3 3c^2 + g}{3c}}\right)$ are saddles.
- (4) When g = 0 and $0 < c < \frac{3}{4}$, system (9) has three singular points $(\pm \sqrt[4]{3c/4}, 0)$ and (0, 0). Furthermore, $(\pm \sqrt[4]{3c/4}, 0)$ are saddles, and (0, 0) is a high-order singular point.
- (5) When g = 0 and $c = \frac{3}{4}$, system (9) has three singular points $(\pm \sqrt{3/4}, 0)$ and (0, 0). Furthermore, $(\pm \sqrt{3/4}, 0)$ are degenerate singular points, and (0, 0) is a high-order singular point.
- (6) When g=0 and $c>\frac{3}{4}$, system (9) has seven singular points $(\pm\sqrt[4]{3c/4},0)$, (0,0), and $(\pm\sqrt{c},\pm\sqrt{\frac{4c^2-3c}{3}})$. Furthermore, $(\pm\sqrt[4]{3c/4},0)$ are centers, (0,0) is a high-order singular point, and $(\pm\sqrt{c},\pm\sqrt{\frac{4c^2-3c}{3}})$ are saddles.
- (7) When $0 < g < 3c^2 4c^3$ and $0 < c < \frac{3}{4}$, system (9) has six singular points $(\pm \varphi_2, 0)$, $(\pm \varphi_3, 0)$ and $(0, \pm \sqrt{\frac{g}{3c}})$, with $0 < \varphi_2 < \sqrt{c} < \varphi_3$. Furthermore, $(\pm \varphi_2, 0)$ and $(\pm \varphi_3, 0)$ are saddles, and $(0, \pm \sqrt{\frac{g}{3c}})$ are nodes.
- (8) When $g = 3c^2 4c^3$ and $0 < c < \frac{1}{4}$, system (9) has six singular points $(\pm \varphi_3, 0)$, $(\pm \sqrt{c}, 0)$ and $(0, \pm \sqrt{\frac{g}{3c}})$, with $\varphi_3 > \sqrt{c}$. Furthermore, $(\pm \varphi_3, 0)$ are saddles, $(\pm \sqrt{c}, 0)$ are degenerate singular points, and $(0, \pm \sqrt{\frac{g}{3c}})$ are nodes.
- (9) When $g = 3c^2 4c^3$ and $\frac{1}{4} < c < \frac{3}{4}$, system (9) has six singular points $(\pm \sqrt{c}, 0)$, $(\pm \varphi_2, 0)$ and $(0, \pm \sqrt{\frac{g}{3c}})$, with $\varphi_2 < \sqrt{c}$. Furthermore $(\pm \sqrt{c}, 0)$ are degenerate singular points, $(\pm \varphi_2, 0)$ are saddles, and $(0, \pm \sqrt{\frac{g}{3c}})$ are nodes.
- (10) When $3c^2 4c^3 < g < c\sqrt{c}$ and $0 < c < \frac{1}{4}$, system (9) has ten singular points $(\pm \varphi_2, 0)$, $(\pm \varphi_3, 0) \left(\pm \sqrt{c}, \pm \sqrt{\frac{4c^3 3c^2 + g}{3c}}\right)$ and $\left(0, \pm \sqrt{\frac{g}{3c}}\right)$, with $\sqrt{c} < \varphi_2 < \varphi_3$. Furthermore, $(\pm \varphi_3, 0)$ and $\left(\pm \sqrt{c}, \pm \sqrt{\frac{4c^3 3c^2 + g}{3c}}\right)$ are saddles, $(\pm \varphi_2, 0)$ are centers, and $\left(0, \pm \sqrt{\frac{g}{3c}}\right)$ are nodes.
- (11) When $\max\{3c^2 4c^3, 0\} < g < c\sqrt{c}$ and $c > \frac{1}{4}$, system (9) has ten singular points $(\pm \varphi_2, 0)$, $(\pm \varphi_3, 0)$, $\left(\pm \sqrt{c}, \pm \sqrt{\frac{4c^3 3c^2 + g}{3c}}\right)$ and $\left(0, \pm \sqrt{\frac{g}{3c}}\right)$, with $0 < \varphi_2 < \varphi_3 < \sqrt{c}$. Furthermore, $(\pm \varphi_2, 0)$ and $\left(\pm \sqrt{c}, \pm \sqrt{\frac{4c^3 3c^2 + g}{3c}}\right)$ are saddles, $(\pm \varphi_3, 0)$ are centers, and $\left(0, \pm \sqrt{\frac{g}{3c}}\right)$ are nodes.
- (12) When $g = c\sqrt{c}$, system (9) has four singular points $(\pm \sqrt[4]{c/4}, 0)$ and $(0, \pm \sqrt{\frac{g}{3c}})$. Furthermore, $(\pm \sqrt[4]{c/4}, 0)$ are degenerate singular points, and $(0, \pm \sqrt{\frac{g}{3c}})$ are nodes.
- (13) When $g > c\sqrt{c}$, system (9) has two singular points $\left(0, \pm \sqrt{\frac{g}{3c}}\right)$. Furthermore, $\left(0, \pm \sqrt{\frac{g}{3c}}\right)$ are nodes.

Note that when g = 0, (0,0) is a high-order singular point of system (9). According to the qualitative theory of differential equations [29], we present the patterns of orbits near (0,0) in Lemma 2.

Lemma 2. When g = 0, (0,0) is a high-order singular point of system (9). Furthermore,

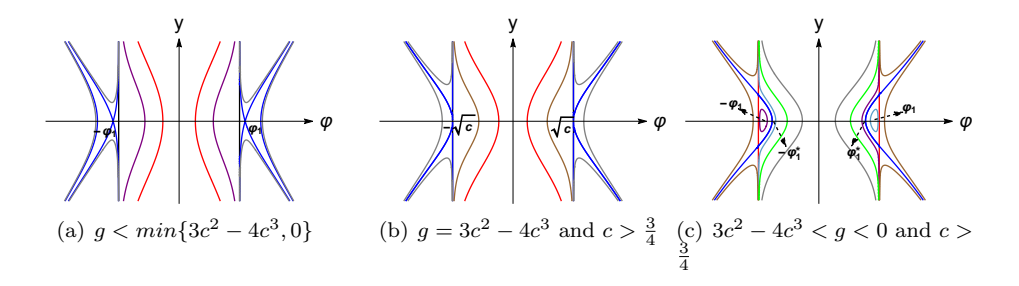


Figure 2. The phase portraits of system (7) when g < 0.

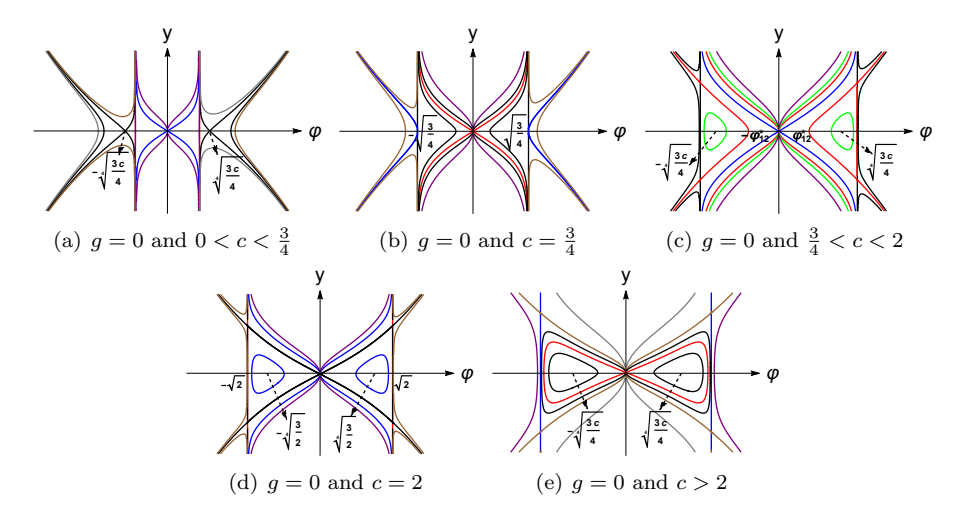


Figure 3. The phase portraits of system (7) when g = 0.

there is an infinite number of orbits tending to (0,0) along $\theta = \frac{\pi}{2}$ and $\theta = \frac{3\pi}{2}$, and there is a unique orbit tending to (0,0) along $\theta = \frac{\pi}{4}, \theta = \frac{3\pi}{4}, \theta = \frac{5\pi}{4}$ and $\theta = \frac{7\pi}{4}$.

Additionally, for the subcase (10) in Lemma 1, when $H_1(\varphi_3,0) = H_1\left(\sqrt{c},\sqrt{\frac{4c^3-3c^2+g}{3c}}\right)$, from which we can obtain a bifurcation value $g=g_1^*$, there exists one orbit connecting $(\varphi_3,0)$ and $\left(\sqrt{c},\sqrt{\frac{4c^3-3c^2+g}{3c}}\right)$. Similarly, when $H_2(\varphi_2,0) = H_2\left(\sqrt{c},\sqrt{\frac{4c^3-3c^2+g}{3c}}\right)$, from which we can obtain a bifurcation value $g=g_2^*$, there exists one orbit connecting $(\varphi_2,0)$ and $\left(\sqrt{c},\sqrt{\frac{4c^3-3c^2+g}{3c}}\right)$, for the subcase (11) in Lemma 1.

Therefore, based on the above analyses, we obtain all possible bifurcations of phase portraits of system (7) in Figures 2, 3, 4, 5, and 6.

Remark 1. Note that when c < 0, system (7) has only one singular line $\varphi = 0$ and $f(\varphi)$ has at most two zeros, which indicates that the phase portraits of system (7) are quite simple and system (7) can only have trivial dynamical behaviors. Therefore, we only focus on the case when c > 0.

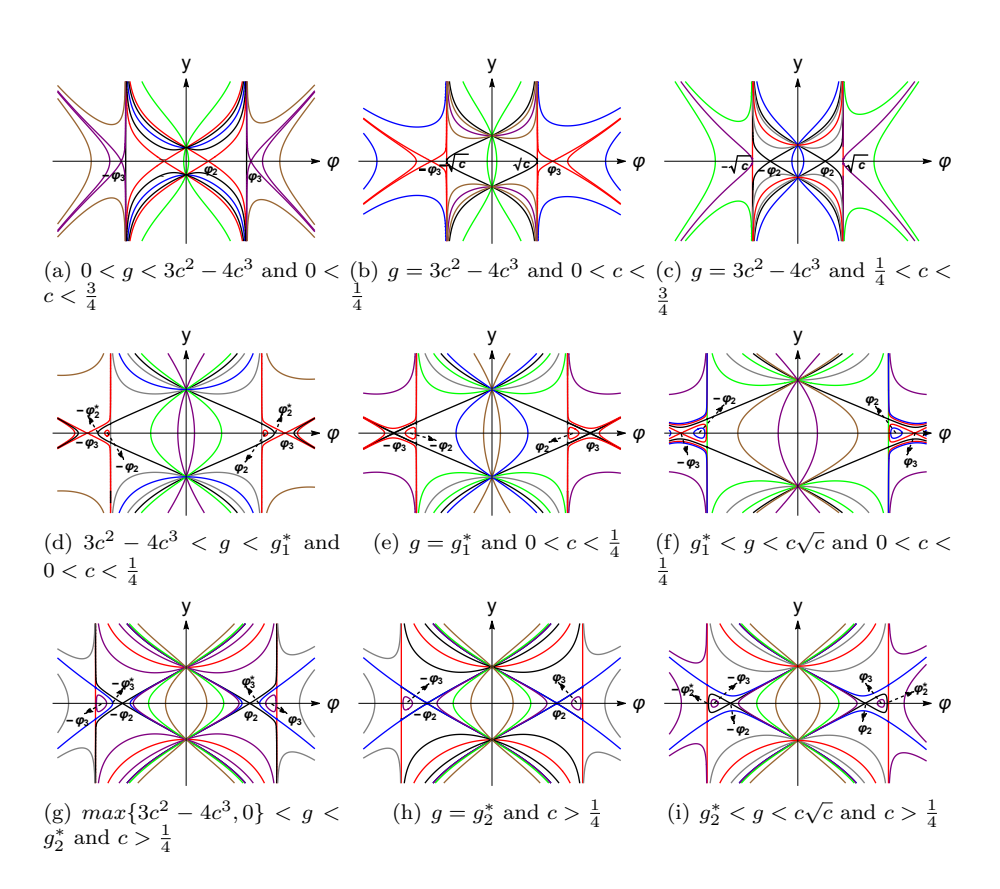


Figure 4. The phase portraits of system (7) when $0 < g < c\sqrt{c}$.

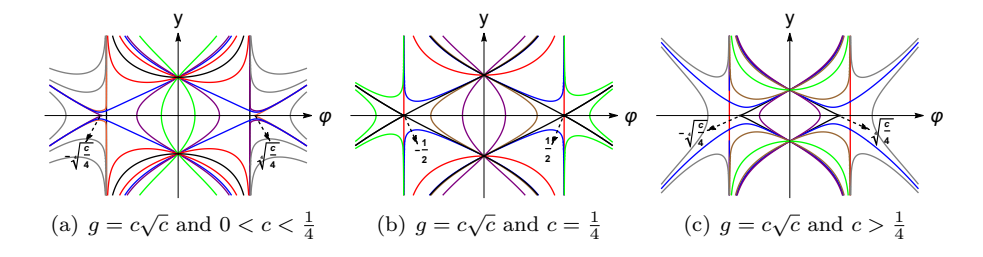


Figure 5. The phase portraits of system (7) when $g = c\sqrt{c}$.

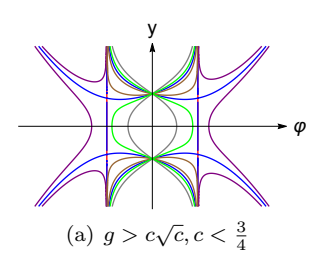


Figure 6. The phase portrait of system (7) when $g > c\sqrt{c}$.

§3 Dynamical behaviors of bounded solutions of system (7)

In this section, we exploit the phase portraits in Figures 2, 3, 4, 5 and 6 to discuss the dynamical behavior of the bounded solutions of system (7), since each orbit (curve) in the phase portraits corresponds to a solution of system (7).

3.1 The case q < 0 (see Figure 2)

(1) For $g < min\{3c^2 - 4c^3, 0\}$ in Figure 2(a).

Corresponding to the four families of orbits, passing through the point $(\varphi_0, 0)$ with $\varphi_0 \in (-\varphi_1, -\sqrt{c}) \bigcup (-\sqrt{c}, 0) \bigcup (0, \sqrt{c}) \bigcup (\sqrt{c}, \varphi_1)$, system (7) has four families of compacton solutions.

Corresponding to the stable and unstable manifolds defined by $H_1(\varphi, y) = H_1(-\varphi_1, 0)$ to the right side of the saddle point $(-\varphi_1, 0)$ and $H_1(\varphi, y) = H_1(\varphi_1, 0)$ to the left side of the saddle point $(\varphi_1, 0)$, system (7) has two pairs of kink-like and antikink-like solutions.

- (2) For $g = 3c^2 4c^3$ and $c > \frac{3}{4}$ in Figure 2(b). Corresponding to the two families of orbits, passing through the point $(\varphi_0, 0)$ with $\varphi_0 \in (-\sqrt{c}, 0) \bigcup (0, \sqrt{c})$, system (7) has two families of compacton solutions.
- (3) For $3c^2 4c^3 < g < 0$ and $c > \frac{3}{4}$ in Figure 2(c).

Corresponding to the two orbits, passing through the point $(-\varphi_1^*, 0)$ defined by $H_2(\varphi, y) = H_2\left(-\sqrt{c}, \sqrt{\frac{4c^3 - 3c^2 + g}{3c}}\right)$ and passing through the point $(\varphi_1^*, 0)$ defined by $H_2(\varphi, y) = H_2\left(\sqrt{c}, \sqrt{\frac{4c^3 - 3c^2 + g}{3c}}\right)$, where φ_1^* is determined by the equation $H_2(\varphi_1^*, 0) = H_2\left(\sqrt{c}, \sqrt{\frac{4c^3 - 3c^2 + g}{3c}}\right)$, system (7) has two periodic cusp wave solutions.

Corresponding to the two families of periodic orbits, around the center point $(-\varphi_1, 0)$ defined by $H_2(\varphi, y) = h_1, h_1 \in \left(H_2\left(-\sqrt{c}, \sqrt{\frac{4c^3 - 3c^2 + g}{3c}}\right), H_2(-\varphi_1, 0)\right)$, and around the center point $(\varphi_1, 0)$ defined by $H_2(\varphi, y) = h_2, h_2 \in \left(H_2(\varphi_1, 0), H_2\left(\sqrt{c}, \sqrt{\frac{4c^3 - 3c^2 + g}{3c}}\right)\right)$, system (7) has two families of periodic wave solutions.

Corresponding to the two families of orbits, passing through the point $(\varphi_0, 0)$ with $\varphi_0 \in (-\varphi_1^*, 0) \bigcup (0, \varphi_1^*)$, system (7) has two families of compacton solutions.

3.2 The case g = 0 (see Figure 3)

(1) For g = 0 and $0 < c < \frac{3}{4}$ in Figure 3(a).

Corresponding to the four families of orbits, passing through the point $(\varphi_0, 0)$ with $\varphi_0 \in \left(-\sqrt[4]{\frac{3c}{4}}, -\sqrt{c}\right) \bigcup (-\sqrt{c}, 0) \bigcup (0, \sqrt{c}) \bigcup \left(\sqrt{c}, \sqrt[4]{\frac{3c}{4}}\right)$, and the two families of orbits,

which are tangent to the y-axis at the point (0,0), system (7) has six families of compacton solutions.

Corresponding to the stable and unstable manifolds defined by $H_1(\varphi, y) = H_1\left(-\sqrt[4]{\frac{3c}{4}}, 0\right)$ to the right side of the saddle point $\left(-\sqrt[4]{\frac{3c}{4}}, 0\right)$, $H_1(\varphi, y) = H_1\left(\sqrt[4]{\frac{3c}{4}}, 0\right)$ to the left side of the saddle point $\left(\sqrt[4]{\frac{3c}{4}}, 0\right)$, and $H_2(\varphi, y) = H_2(0, 0)$ to the left and right sides of the high-order singular point (0,0) (the orbits tending to (0,0) along $\theta = \frac{\pi}{4}, \theta = \frac{3\pi}{4}, \theta = \frac{5\pi}{4}$ and $\theta = \frac{7\pi}{4}$), system (7) has four pairs of kink-like and antikink-like solutions.

(2) For g = 0 and $c = \frac{3}{4}$ in Figure 3(b).

Corresponding to the two families of orbits, passing through the point $(\varphi_0, 0)$ with $\varphi_0 \in (-\sqrt{3/4}, 0) \bigcup (0, \sqrt{3/4})$, and the two families of orbits, which are tangent to the y-axis at the point (0,0), system (7) has four families of compacton solutions.

Corresponding to the stable and unstable manifolds defined by $H_2(\varphi, y) = H_2(0, 0)$ to the left and right sides of the high-order singular point (0,0) (the orbits tending to (0,0) along $\theta = \frac{\pi}{4}, \theta = \frac{3\pi}{4}, \theta = \frac{5\pi}{4}$ and $\theta = \frac{7\pi}{4}$), system (7) has two pairs of kink-like and antikink-like solutions.

(3) For g = 0 and $\frac{3}{4} < c < 2$ in Figure 3(c).

Corresponding to the two orbits, passing through the point $(-\varphi_{12}^*, 0)$ defined by $H_2(\varphi, y) = H_2\left(-\sqrt{c}, \sqrt{\frac{4c^2-3c}{3}}\right)$ and passing through the point $(\varphi_{12}^*, 0)$ defined by $H_2(\varphi, y) = H_2\left(\sqrt{c}, \sqrt{\frac{4c^2-3c}{3}}\right)$, where φ_{12}^* is determined by $H_2(\varphi_{12}^*, 0) = H_2\left(\sqrt{c}, \sqrt{\frac{4c^2-3c}{3}}\right)$, system (7) has two periodic cusp wave solutions, which are illustrated in Figure 7(a).

Corresponding to the two families of periodic orbits, around the center point $\left(-\sqrt[4]{\frac{3c}{4}},0\right)$ defined by $H_2(\varphi,y)=h_1,h_1\in \left(H_2\left(-\sqrt{c},\sqrt{\frac{4c^2-3c}{3}}\right),H_2\left(-\sqrt[4]{\frac{3c}{4}},0\right)\right)$, and around the center point $\left(\sqrt[4]{\frac{3c}{4}},0\right)$ defined by $H_2(\varphi,y)=h_2,h_2\in \left(H_2(\sqrt[4]{\frac{3c}{4}},0),H_2\left(\sqrt{c},\sqrt{\frac{4c^2-3c}{3}}\right)\right)$, system (7) has two families of periodic wave solutions.

Corresponding to the two families of orbits, passing through the point $(\varphi_0, 0)$ with $\varphi_0 \in (-\varphi_{12}^*, 0) \bigcup (0, \varphi_{12}^*)$, and the two families of orbits, which are tangent to the y-axis at the point (0, 0), system (7) has four families of compacton solutions.

Corresponding to the stable and unstable manifolds defined by $H_2(\varphi, y) = H_2(0,0)$ to the left and right sides of the high-order singular point (0,0) (the orbits tending to (0,0) along $\theta = \frac{\pi}{4}, \theta = \frac{3\pi}{4}, \theta = \frac{5\pi}{4}$ and $\theta = \frac{7\pi}{4}$), system (7) has two pairs of kink-like and antikink-like solutions.

(4) For g = 0 and c = 2 in Figure 3(d).

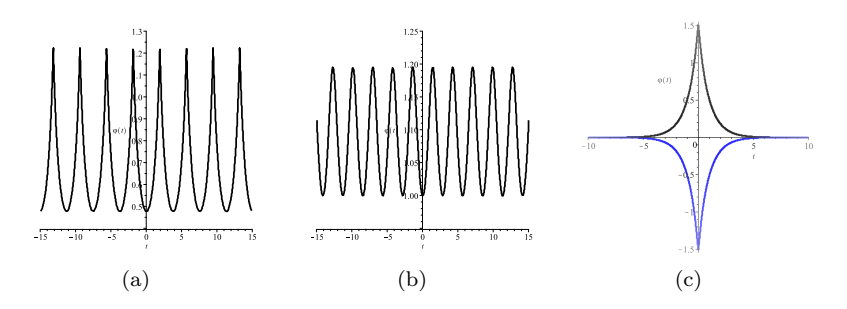


Figure 7. The profiles of periodic cusp wave solution, periodic wave solution and solitary wave solutions of Eq.(2).

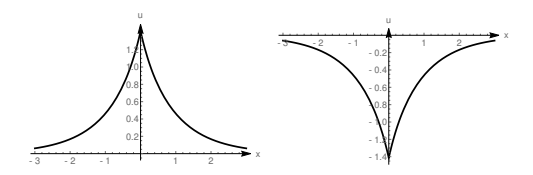


Figure 8. The profiles of peakons (15) and (16).

Corresponding to the two triangle orbits, passing through the point (0,0) defined by $H_2(\varphi, y) = 0$, which has expressions

$$y = \pm \sqrt{\frac{\varphi^4 + 3\varphi^2}{3}}, \ 0 \le |\varphi| < \sqrt{2}, \tag{12}$$

and

$$\varphi = \pm \sqrt{2}, \ |y| \le \sqrt{\frac{10}{3}}.$$

Substituting (12) into the first equation of (7) and integrating along the triangle orbits, we have

$$\int_{\varphi}^{\sqrt{2}} \frac{\sqrt{3}}{\sqrt{\varphi^4 + 3\varphi^2}} d\varphi = |\xi|, \text{ for } 0 \le \varphi < \sqrt{2}, \tag{13}$$

and

$$\int_{-\sqrt{2}}^{\varphi} \frac{\sqrt{3}}{\sqrt{\varphi^4 + 3\varphi^2}} d\varphi = -|\xi|, \text{ for } -\sqrt{2} < \varphi \le 0.$$
 (14)

From (13) and (14), we immediately obtain the peakons

$$u(x,t) = \frac{6}{\frac{1}{\theta} \exp^{|x-2t|} - 3\theta \exp^{-|x-2t|}},$$
(15)

and

$$u(x,t) = -\frac{6}{\frac{1}{\theta} \exp^{|x-2t|} - 3\theta \exp^{-|x-2t|}},$$
(16)

where

$$\theta = \frac{\sqrt{2}}{\sqrt{15} + 3},$$

 $\theta = \frac{\sqrt{2}}{\sqrt{15} + 3},$ the profiles of which are given in Figures 8(a) and 8(b).

Corresponding to the two families of periodic orbits, around the center point $(-\sqrt[4]{3/2},0)$

defined by $H_2(\varphi, y) = h_1, h_1 \in (H_2(0,0), H_2(-\sqrt[4]{3/2}, 0))$, and around the center point $(\sqrt[4]{3/2}, 0)$ defined by $H_2(\varphi, y) = h_2, h_2 \in (H_2(\sqrt[4]{3/2}, 0), H_2(0, 0))$, system (7) has two families of periodic wave solutions. We illustrate the profile of one periodic wave solution in Figure 7(b).

Corresponding to the two families of orbits, which are tangent to the y-axis at the point (0,0), system (7) has two families of compacton solutions.

(5) For g = 0 and c > 2 in Figure 3(e).

Corresponding to the two homoclinic orbits to the point (0,0), which tend to (0,0) along $\theta = \frac{\pi}{4}$, $\theta = \frac{3\pi}{4}$, $\theta = \frac{5\pi}{4}$ and $\theta = \frac{7\pi}{4}$, defined by $H_2(\varphi, y) = 0$, system (7) has two solitary wave solutions, which are illustrated in Figure 7(c).

Corresponding to the two families of periodic orbits, around the center point $\left(-\sqrt[4]{\frac{3c}{4}},0\right)$ defined by $H_2(\varphi,y)=h_1,h_1\in \left(H_2(0,0),H_2\left(-\sqrt[4]{\frac{3c}{4}},0\right)\right)$, and around the center point $\left(\sqrt[4]{\frac{3c}{4}},0\right)$ defined by $H_2(\varphi,y)=h_2,h_2\in \left(H_2\left(\sqrt[4]{\frac{3c}{4}},0\right),H_2(0,0)\right)$, and the two families of homoclinic orbits, which are tangent to y-axis at the point (0,0), system (7) has four families of periodic wave solutions.

Corresponding to the two orbits, passing through the point (0,0) defined by $H_2(0,0) = H_2\left(\pm\sqrt{c},\sqrt{\frac{4c^2-3c}{3}}\right)$, system (7) has two periodic cusp wave solutions.

Corresponding to the two families of orbits, which are tangent to the y-axis at the point (0,0), system (7) has two families of compacton solutions.

3.3 The case $0 < g < c\sqrt{c}$ (see Figure 4)

(1) For $0 < g < 3c^2 - 4c^3$ and $0 < c < \frac{3}{4}$ in Figure 4(a).

Corresponding to the six families of orbits, passing through the point $(\varphi_0, 0)$ with $\varphi_0 \in (-\varphi_3, -\sqrt{c}) \bigcup (-\sqrt{c}, -\varphi_2) \bigcup (-\varphi_2, 0) \bigcup (0, \varphi_2) \bigcup (\varphi_2, \sqrt{c}) \bigcup (\sqrt{c}, \varphi_3)$, and the two families of orbits, passing through the points $(0, \pm \sqrt{\frac{g}{3c}})$ defined by $H_2(\varphi, y) = h_2$, $h_2 \in (H_2(\varphi_2, 0), H_2(-\varphi_2, 0))$, system (7) has eight families of compacton solutions.

Corresponding to the stable and unstable manifolds defined by $H_1(\varphi, y) = H_1(-\varphi_3, 0)$ to the right side of the saddle point $(-\varphi_3, 0)$, $H_2(\varphi, y) = H_2(-\varphi_2, 0)$ to the left and right sides of the saddle point $(-\varphi_2, 0)$, $H_2(\varphi, y) = H_2(\varphi_2, 0)$ to the left and right sides of the saddle point $(\varphi_2, 0)$, and $H_1(\varphi, y) = H_1(\varphi_3, 0)$ to the left side of the saddle point $(\varphi_3, 0)$, system (7) has six pairs of kink-like and antikink-like solutions.

(2) For $g = 3c^2 - 4c^3$ and $0 < c < \frac{1}{4}$ in Figure 4(b).

Corresponding to the four families of orbits, passing through the point $(\varphi_0, 0)$ with $\varphi_0 \in (-\varphi_3, -\sqrt{c}) \bigcup [-\sqrt{c}, 0) \bigcup (0, \sqrt{c}] \bigcup (\sqrt{c}, \varphi_3)$, and the two families of orbits, passing through the points $(0, \pm \sqrt{\frac{g}{3c}})$ defined by $H_2(\varphi, y) = h_2$, $h_2 \in (H_2(\sqrt{c}, 0), H_2(-\sqrt{c}, 0))$, system (7) has six families of compacton solutions.

Corresponding to the stable and unstable manifolds defined by $H_1(\varphi, y) = H_1(-\varphi_3, 0)$ to the right side of the saddle point $(-\varphi_3, 0)$ and $H_1(\varphi, y) = H_1(\varphi_3, 0)$ to the left side of the saddle point $(\varphi_3, 0)$, system (7) has two pairs of kink-like and antikink-like solutions.

(3) For $g = 3c^2 - 4c^3$ and $\frac{1}{4} < c < \frac{3}{4}$ in Figure 4(c).

Corresponding to the four families of orbits, passing through the point $(\varphi_0, 0)$ with $\varphi_0 \in (-\sqrt{c}, -\varphi_2) \bigcup (-\varphi_2, 0) \bigcup (0, \varphi_2) \bigcup (\varphi_2, \sqrt{c})$, and the two families of orbits, passing through the points $(0, \pm \sqrt{\frac{g}{3c}})$ defined by $H_2(\varphi, y) = h_2$, $h_2 \in (H_2(\varphi_2, 0), H_2(-\varphi_2, 0))$, system (7) has six families of compacton solutions.

Corresponding to the stable and unstable manifolds defined by $H_2(\varphi, y) = H_2(-\varphi_2, 0)$ to the left and right sides of the saddle point $(-\varphi_2, 0)$ and $H_2(\varphi, y) = H_2(\varphi_2, 0)$ to the left and right sides of the saddle point $(\varphi_2, 0)$, system (7) has four pairs of kink-like and antikink-like solutions.

(4) For $3c^2 - 4c^3 < g < g_1^*$ and $0 < c < \frac{1}{4}$ in Figure 4(d).

Corresponding to the two orbits, passing through the point $(-\varphi_2^*, 0)$ defined by $H_1(\varphi, y) = H_1\left(-\sqrt{c}, \sqrt{\frac{4c^3 - 3c^2 + g}{3c}}\right)$ and passing through the point $(\varphi_2^*, 0)$ defined by $H_1(\varphi, y) = H_1\left(\sqrt{c}, \sqrt{\frac{4c^3 - 3c^2 + g}{3c}}\right)$, where φ_2^* is determined by the equation $H_1(\varphi_2^*, 0) = H_1\left(\sqrt{c}, \sqrt{\frac{4c^3 - 3c^2 + g}{3c}}\right)$, system (7) has two periodic cusp wave solutions.

Corresponding to the two families of periodic orbits, around the center point $(-\varphi_2, 0)$ defined by $H_1(\varphi, y) = h_1, h_1 \in \left(H_1(-\varphi_2, 0), H_1\left(-\sqrt{c}, \sqrt{\frac{4c^3 - 3c^2 + g}{3c}}\right)\right)$, and around the center point $(\varphi_2, 0)$ defined by $H_1(\varphi, y) = h_2, h_2 \in \left(H_1\left(\sqrt{c}, \sqrt{\frac{4c^3 - 3c^2 + g}{3c}}\right), H_1(\varphi_2, 0)\right)$, system (7) has two families of periodic wave solutions.

Corresponding to the four families of orbits, passing through the point $(\varphi_0, 0)$ with $\varphi_0 \in (-\varphi_3, -\varphi_2^*) \bigcup (-\sqrt{c}, 0) \bigcup (0, \sqrt{c}) \bigcup (\varphi_2^*, \varphi_3)$, and the two families of orbits, passing through the points $(0, \pm \sqrt{\frac{g}{3c}})$ defined by $H_2(\varphi, y) = h_2$,

the points $(0, \pm \sqrt{\frac{g}{3c}})$ defined by $H_2(\varphi, y) = h_2$, $h_2 \in \left(H_2\left(\sqrt{c}, \sqrt{\frac{4c^3 - 3c^2 + g}{3c}}\right), H_2\left(-\sqrt{c}, \sqrt{\frac{4c^3 - 3c^2 + g}{3c}}\right)\right)$, system (7) has six families of compacton solutions.

Corresponding to the stable and unstable manifolds defined by $H_1(\varphi, y) = H_1(-\varphi_3, 0)$ to the right side of the saddle point $(-\varphi_3, 0)$ and $H_1(\varphi, y) = H_1(\varphi_3, 0)$ to the left side of the saddle point $(\varphi_3, 0)$, system (7) has two pairs of kink-like and antikink-like solutions.

(5) For $g = g_1^*$ and $0 < c < \frac{1}{4}$ in Figure 4(e).

Corresponding to the two triangle orbits, passing through the point $(-\varphi_3, 0)$ defined by $H_1(\varphi, y) = H_1\left(-\sqrt{c}, \sqrt{\frac{4c^3 - 3c^2 + g_1^*}{3c}}\right)$, and passing through the point $(\varphi_3, 0)$ defined by

 $H_1(\varphi, y) = H_1\left(\sqrt{c}, \sqrt{\frac{4c^3 - 3c^2 + g_1^*}{3c}}\right)$, where φ_3 is determined by the equation $H_1(\varphi_3, 0) = H_1\left(\sqrt{c}, \sqrt{\frac{4c^3 - 3c^2 + g_1^*}{3c}}\right)$ system (7) has two peakons.

Corresponding to the two families of periodic orbits, around the center point $(-\varphi_2, 0)$ defined by $H_1(\varphi, y) = h_1, h_1 \in \left(H_1(-\varphi_2, 0), H_1\left(-\sqrt{c}, \sqrt{\frac{4c^3 - 3c^2 + g_1^*}{3c}}\right)\right)$, and around the center point $(\varphi_2, 0)$ defined by $H_1(\varphi, y) = h_2, h_2 \in \left(H_1\left(\sqrt{c}, \sqrt{\frac{4c^3 - 3c^2 + g_1^*}{3c}}\right), H_1(\varphi_2, 0)\right)$, system (7) has two families of periodic wave solutions.

Corresponding to the two families of orbits, passing through the point $(\varphi_0,0)$ with $\varphi_0 \in (-\sqrt{c},0) \bigcup (0,\sqrt{c})$, and the two families of orbits, passing through the points $\left(0,\pm\sqrt{\frac{g_1^*}{3c}}\right)$ defined by $H_2(\varphi,y)=h_2$, $h_2\in \left(H_2\left(\sqrt{c},\sqrt{\frac{4c^3-3c^2+g_1^*}{3c}}\right),H_2\left(-\sqrt{c},\sqrt{\frac{4c^3-3c^2+g_1^*}{3c}}\right)\right)$, system (7) has four families of compacton solutions.

(6) For $g_1^* < g < c\sqrt{c}$ and $0 < c < \frac{1}{4}$ in Figure 4(f).

Corresponding to the two homoclinic orbits to the saddle points $(-\varphi_3, 0)$ defined by $H_1(\varphi, y) = H_1(-\varphi_3, 0)$ and the saddle points $(\varphi_3, 0)$ defined by $H_1(\varphi, y) = H_1(\varphi_3, 0)$, system (7) has two solitary wave solutions.

Corresponding to the two families of periodic orbits, around the center point $(-\varphi_2, 0)$ defined by $H_1(\varphi, y) = h_1, h_1 \in (H_1(-\varphi_2, 0), H_1(-\varphi_3, 0))$, and around the center point $(\varphi_2, 0)$ defined by $H_1(\varphi, y) = h_2, h_2 \in (H_1(\varphi_3, 0), H_1(\varphi_2, 0))$, system (7) has two families of periodic wave solutions.

Corresponding to the two families of orbits, passing through the point $(\varphi_0, 0)$ with $\varphi_0 \in (-\sqrt{c}, 0) \bigcup (0, \sqrt{c})$, and the two families of orbits, passing through the points $(0, \pm \sqrt{\frac{g}{3c}})$ defined by $H_2(\varphi, y) = h_2$,

 $h_2 \in \left(H_2\left(\sqrt{c}, \sqrt{\frac{4c^3 - 3c^2 + g}{3c}}\right), H_2\left(-\sqrt{c}, \sqrt{\frac{4c^3 - 3c^2 + g}{3c}}\right)\right)$, system (7) has four families of compacton solutions.

(7) For $max\{3c^2 - 4c^3, 0\} < g < g_2^*$ and $c > \frac{1}{4}$ in Figure 4(g).

Corresponding to the two family of orbits, passing through the point $(-\varphi_3^*, 0)$ defined by $H_2(\varphi, y) = H_2\left(-\sqrt{c}, \sqrt{\frac{4c^3 - 3c^2 + g}{3c}}\right)$ and passing through the point $(\varphi_3^*, 0)$ defined by $H_2(\varphi, y) = H_2\left(\sqrt{c}, \sqrt{\frac{4c^3 - 3c^2 + g}{3c}}\right)$, where φ_3^* is determined by the equation $H_2(\varphi_3^*, 0) = H_2\left(\sqrt{c}, \sqrt{\frac{4c^3 - 3c^2 + g}{3c}}\right)$, system (7) has two periodic cusp wave solutions.

Corresponding to the two families of periodic orbits, around the center point $(-\varphi_3, 0)$ defined by $H_2(\varphi, y) = h_1, h_1 \in \left(H_2\left(-\sqrt{c}, \sqrt{\frac{4c^3 - 3c^2 + g}{3c}}\right), H_2(-\varphi_3, 0)\right)$, and around the

center point $(\varphi_3, 0)$ defined by $H_2(\varphi, y) = h_2, h_2 \in \left(H_2(\varphi_3, 0), H_2\left(\sqrt{c}, \sqrt{\frac{4c^3 - 3c^2 + g}{3c}}\right)\right)$, system (7) has two families of periodic wave solutions.

Corresponding to the four families of orbits, passing through the point $(\varphi_0, 0)$ with $\varphi_0 \in (-\varphi_3^*, -\varphi_2) \bigcup (-\varphi_2, 0) \bigcup (0, \varphi_2) \bigcup (\varphi_2, \varphi_3^*)$, and the two families of orbits, passing through the points $(0, \pm \sqrt{\frac{g}{3c}})$ defined by $H_2(\varphi, y) = h_2$, $h_2 \in (H_2(\varphi_2, 0), H_2(-\varphi_2, 0))$, system (7) has six families of compacton solutions.

Corresponding to the stable and unstable manifolds defined by $H_2(\varphi, y) = H_2(-\varphi_2, 0)$ to the left and right sides of the saddle point $(-\varphi_2, 0)$ and $H_2(\varphi, y) = H_2(\varphi_2, 0)$ to the left and right sides of the saddle point $(\varphi_2, 0)$, system (7) has four pairs of kink-like and antikink-like solutions.

(8) For $g = g_2^*$ and $c > \frac{1}{4}$ in Figure 4(h).

Corresponding to the two triangle orbits, passing through the point $(-\varphi_2,0)$ defined by $H_2(\varphi,y)=H_2\left(-\sqrt{c},\sqrt{\frac{4c^3-3c^2+g_2^*}{3c}}\right)$, and passing through the point $(\varphi_2,0)$ defined by $H_2(\varphi,y)=H_2\left(\sqrt{c},\sqrt{\frac{4c^3-3c^2+g_2^*}{3c}}\right)$, where φ_2 is determined by the equation $H_2(\varphi_2,0)=H_2\left(\sqrt{c},\sqrt{\frac{4c^3-3c^2+g_2^*}{3c}}\right)$ system (7) has two peakon solutions.

Corresponding to the two families of periodic orbits, around the center point $(-\varphi_3, 0)$ defined by $H_2(\varphi, y) = h_1, h_1 \in \left(H_2\left(-\sqrt{c}, \sqrt{\frac{4c^3 - 3c^2 + g_2^*}{3c}}\right), H_2(-\varphi_3, 0)\right)$, and around the center point $(\varphi_3, 0)$ defined by $H_2(\varphi, y) = h_2, h_2 \in \left(H_2(\varphi_3, 0), H_2\left(\sqrt{c}, \sqrt{\frac{4c^3 - 3c^2 + g_2^*}{3c}}\right)\right)$, system (7) has two families of periodic wave solutions.

Corresponding to the two families of orbits, passing through the point $(\varphi_0, 0)$ with $\varphi_0 \in (-\varphi_2, 0) \bigcup (0, \varphi_2)$, and the two families of orbits, passing through the points $\left(0, \pm \sqrt{\frac{g_2^*}{3c}}\right)$ defined by $H_2(\varphi, y) = h_2$, $h_2 \in (H_2(\varphi_2, 0), H_2(-\varphi_2, 0))$, system (7) has four families of compacton solutions.

Corresponding to the stable and unstable manifolds defined by $H_2(\varphi, y) = H_2(-\varphi_2, 0)$ to the right side of the saddle point $(-\varphi_2, 0)$ and $H_2(\varphi, y) = H_2(\varphi_2, 0)$ to the left side of the saddle point $(\varphi_2, 0)$, system (7) has two pairs of kink-like and antikink-like solutions.

(9) For $g_2^* < g < c\sqrt{c}$ and $c > \frac{1}{4}$ in Figure 4(i).

Corresponding to the two homoclinic orbits to the saddle points $(-\varphi_2, 0)$ defined by $H_2(\varphi, y) = H_2(-\varphi_2, 0)$ and the saddle points $(\varphi_2, 0)$ defined by $H_2(\varphi, y) = H_2(\varphi_2, 0)$, system (7) has two solitary wave solutions.

Corresponding to the two family of periodic orbits, around the center point $(-\varphi_3, 0)$ defined by $H_2(\varphi, y) = h_1, h_1 \in (H_2(-\varphi_2, 0), H_2(-\varphi_3, 0))$, and around the center point $(\varphi_3, 0)$ defined by $H_2(\varphi, y) = h_2, h_2 \in (H_2(\varphi_3, 0), H_2(\varphi_2, 0))$, system (7) has two families of periodic wave solutions.

Corresponding to the four families of orbits, passing through the point $(\varphi_0,0)$ with $\varphi_0 \in (-\sqrt{c}, -\varphi_2^*) \bigcup (-\varphi_2, 0) \bigcup (0, \varphi_2) \bigcup (\varphi_2^*, \sqrt{c})$, where φ_2^* is determined by the equation $H_2(\varphi_2^*, 0) = H_2(\varphi_2, 0)$, and the two families of orbits, passing through the points $(0, \pm \sqrt{\frac{g}{3c}})$ defined by $H_2(\varphi, y) = h_2$, $h_2 \in (H_2(\varphi_2, 0), H_2(-\varphi_2, 0))$, system (7) has six families of compacton solutions.

Corresponding to the stable and unstable manifolds defined by $H_2(\varphi, y) = H_2(-\varphi_2, 0)$ to the right side of the saddle point $(-\varphi_2, 0)$ and $H_2(\varphi, y) = H_2(\varphi_2, 0)$ to the left side of the saddle point $(\varphi_2, 0)$, system (7) has two pairs of kink-like and antikink-like solutions.

3.4 The case $g = c\sqrt{c}$ (see Figure 5)

(1) For $g = c\sqrt{c}$ and $0 < c < \frac{1}{4}$ in Figure 5(a).

Corresponding to the two families of orbits, passing through the point $(\varphi_0,0)$ with $\varphi_0 \in (-\sqrt{c},0) \bigcup (0,\sqrt{c})$, and the two families of orbits, passing through the points $\left(0,\pm\sqrt{\frac{\sqrt{c}}{3}}\right)$ defined by $H_2(\varphi,y)=h_2$, $h_2\in \left(H_2\left(\sqrt{c},\sqrt{\frac{4c^2-3c+\sqrt{c}}{3}}\right),H_2\left(-\sqrt{c},\sqrt{\frac{4c^2-3c+\sqrt{c}}{3}}\right)\right)$, system (7) has four families of compacton solutions.

(2) For $g = c\sqrt{c}$ and $c = \frac{1}{4}$ in Figure 5(b).

Corresponding to the two families of orbits, passing through the point $(\varphi_0, 0)$ with $\varphi_0 \in (-\frac{1}{2}, 0) \bigcup (0, \frac{1}{2})$, and the two families of orbits, passing through the points $\left(0, \pm \sqrt{\frac{1}{6}}\right)$ defined by $H_2(\varphi, y) = h_2$, $h_2 \in \left(H_2\left(\frac{1}{4}, 0\right), H_2\left(-\frac{1}{4}, 0\right)\right)$, system (7) has four families of compacton solutions.

(3) For $g = c\sqrt{c}$ and $c > \frac{1}{4}$ in Figure 5(c).

Corresponding to the four families of orbits, passing through the point $(\varphi_0, 0)$ with $\varphi_0 \in (-\sqrt{c}, -\sqrt[4]{\frac{c}{4}}) \bigcup (-\sqrt[4]{\frac{c}{4}}, 0) \bigcup (0, \sqrt[4]{\frac{c}{4}}) \bigcup (\sqrt[4]{\frac{c}{4}}, \sqrt{c})$, and the two families of orbits, passing through the points $\left(0, \pm \sqrt{\frac{\sqrt{c}}{3}}\right)$ defined by $H_2(\varphi, y) = h_2$,

through the points
$$\left(0, \pm \sqrt{\frac{\sqrt{c}}{3}}\right)$$
 defined by $H_2(\varphi, y) = h_2$, $h_2 \in \left(H_2\left(\sqrt{c}, \sqrt{\frac{4c^2 - 3c + \sqrt{c}}{3}}\right), H_2\left(-\sqrt{c}, \sqrt{\frac{4c^2 - 3c + \sqrt{c}}{3}}\right)\right)$, system (7) has six families of compacton solutions.

Corresponding to the stable and unstable manifolds defined by $H_2(\varphi, y) = H_2(-\sqrt[4]{\frac{c}{4}}, 0)$ to the right side of the saddle point $(-\sqrt[4]{\frac{c}{4}}, 0)$ and $H_2(\varphi, y) = H_2(\sqrt[4]{\frac{c}{4}}, 0)$ to the left side of the saddle point $(\sqrt[4]{\frac{c}{4}}, 0)$, system (7) has two pairs of kink-like and antikink-like solutions.

3.5 The case $g > c\sqrt{c}$ (see Figure 6)

Corresponding to the two families of orbits, passing through the point $(\varphi_0, 0)$ with $\varphi_0 \in (-\sqrt{c}, 0) \bigcup (0, \sqrt{c})$, and the two families of orbits, passing through the points $(0, \pm \sqrt{\frac{g}{3c}})$ defined

by $H_2(\varphi, y) = h_2, h_2 \in \left(H_2\left(\sqrt{c}, \sqrt{\frac{4c^3 - 3c^2 + g}{3c}}\right), H_2\left(-\sqrt{c}, \sqrt{\frac{4c^3 - 3c^2 + g}{3c}}\right)\right)$, system (7) has four families of compacton solutions.

§4 Main results

Based on the above results, we summarize the main results about different profiles for the wave function $\varphi(\xi)$ and their dynamical behaviors under different parameter conditions in Theorems 1–5.

Theorem 1. Under the condition g < 0, the following conclusions hold.

- (1) When $g < min\{3c^2 4c^3, 0\}$, Eq.(2) has four families of compacton solutions and two pairs of kink-like and antikink-like solutions.
- (2) When $g = 3c^2 4c^3$ and $c > \frac{3}{4}$, Eq.(2) has two families of compacton solutions.
- (3) When $3c^2 4c^3 < g < 0$ and $c > \frac{3}{4}$, Eq.(2) has two periodic cusp wave solutions, two families of periodic wave solutions, and two families of compacton solutions.

Theorem 2. Under the condition g = 0, the following conclusions hold.

- (1) When g = 0 and $0 < c < \frac{3}{4}$, Eq.(2) has six families of compacton solutions and four pairs of kink-like and antikink-like solutions.
- (2) When g = 0 and $c = \frac{3}{4}$, Eq.(2) has four families of compacton solutions and two pairs of kink-like and antikink-like solutions.
- (3) When g = 0 and $\frac{3}{4} < c < 2$, Eq.(2) has two periodic cusp wave solutions, two families of periodic wave solutions, four families of compacton solutions, and two pairs of kink-like and antikink-like solutions.
- (4) When g = 0 and c = 2, Eq.(2) has the peakons with exact explicit expressions (15) and (16), two families of periodic wave solutions, and two families of compacton solutions.
- (5) When g = 0 and c > 2, Eq.(2) has two solitary wave solutions, four families of periodic wave solutions, two periodic cusp wave solutions, and two families of compacton solutions.

Theorem 3. Under the condition $0 < g < c\sqrt{c}$, the following conclusions hold.

- (1) When $0 < g < 3c^2 4c^3$ and $0 < c < \frac{3}{4}$, Eq.(2) has eight families of compacton solutions and six pairs of kink-like and antikink-like solutions.
- (2) When $g = 3c^2 4c^3$ and $0 < c < \frac{1}{4}$, Eq.(2) has six families of compacton solutions and two pairs of kink-like and antikink-like solutions.
- (3) When $g = 3c^2 4c^3$ and $\frac{1}{4} < c < \frac{3}{4}$, Eq.(2) has six families of compacton solutions and four pairs of kink-like and antikink-like solutions.

- (4) When $3c^2 4c^3 < g < g_1^*$ and $0 < c < \frac{1}{4}$, Eq.(2) has two periodic cusp wave solutions, two families of periodic wave solutions, six families of compacton solutions, and two pairs of kink-like and antikink-like solutions.
- (5) When $g = g_1^*$ and $0 < c < \frac{1}{4}$, Eq.(2) has two peakons, two families of periodic wave solutions, and four families of compacton solutions.
- (6) When $g_1^* < g < c\sqrt{c}$ and $0 < c < \frac{1}{4}$, Eq.(2) has two solitary wave solutions, two families of periodic wave solutions, and four families of compacton solutions.
- (7) When $\max\{3c^2-4c^3,0\} < g < g_2^*$ and $c > \frac{1}{4}$, Eq.(2) has two periodic cusp wave solutions, two families of periodic wave solutions, six families of compacton solutions, and four pairs of kink-like and antikink-like solutions.
- (8) When $g = g_2^*$ and $c > \frac{1}{4}$, Eq.(2) has two peakon solutions, two families of periodic wave solutions, four families of compacton solutions, and two pairs of kink-like and antikink-like solutions.
- (9) When $g_2^* < g < c\sqrt{c}$ and $c > \frac{1}{4}$, Eq.(2) has two solitary wave solutions, two families of periodic wave solutions, six families of compacton solutions, and two pairs of kink-like and antikink-like solutions.

Theorem 4. Under the condition $g = c\sqrt{c}$, the following conclusions hold.

- (1) When $g = c\sqrt{c}$ and $0 < c < \frac{1}{4}$, Eq.(2) has four families of compacton solutions.
- (2) When $g = c\sqrt{c}$ and $c = \frac{1}{4}$, Eq.(2) has four families of compacton solutions.
- (3) When $g = c\sqrt{c}$ and $c > \frac{1}{4}$, Eq.(2) has six families of compacton solutions and two pairs of kink-like and antikink-like solutions.

Theorem 5. Under the condition $g > c\sqrt{c}$, Eq.(2) has four families of compacton solutions.

Remark 2. In the previous works, peakons and periodic cusp waves were not found. In addition, we confirm the abundant dynamical behaviors of bounded traveling wave solutions under different parameter conditions. Therefore, the present work extends the results about Eq.(2) [15–17].

§5 Numerical simulations

In this section, we numerically simulate the solutions of the subcase when $0 < g < 3c^2 - 4c^3$ and $0 < c < \frac{3}{4}$.

Taking c = 0.5 and $g = 0.125 \in (0, 3c^2 - 4c^3)$, which indicates that $\varphi_2 = 0.259781$, $\sqrt{c} = 0.707$, $\varphi_3 = 0.758837$, we illustrate the profiles of the compacton solutions $\varphi(\xi)$ in Figures 9(a) and 9(b) by taking the initial point (φ_0, y_0) with $\varphi_0 = -0.75, y_0 = 0$, $\varphi_0 = -0.4, y_0 = 0$, $\varphi_0 = -0.1, y_0 = 0$, $\varphi_0 = 0.1, y_0 = 0$, $\varphi_0 = 0.4, y_0 = 0$, $\varphi_0 = 0.75, y_0 = 0$, and $\varphi_0 = 0.1, y_0 = 0$, $\varphi_0 = 0.1, y_0 =$

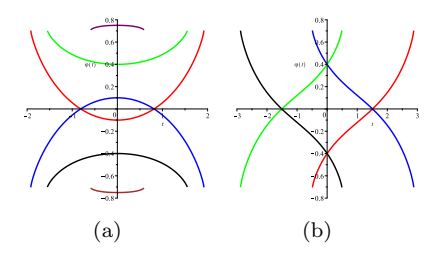


Figure 9. The compacton solutions of Eq.(2) when $0 < g < 3c^2 - 4c^3$ and $0 < c < \frac{3}{4}$.

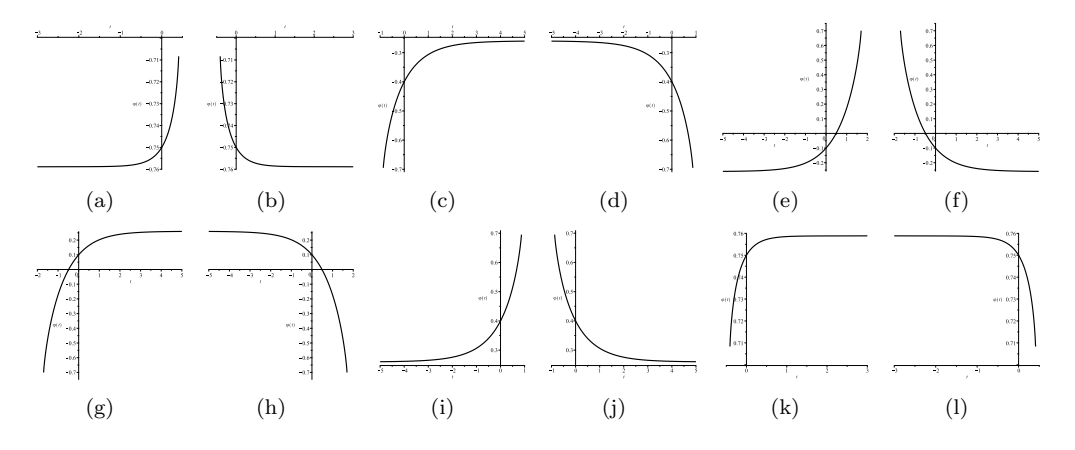


Figure 10. The six pairs of kink-like and antikink-like solutions of Eq.(2) when $0 < g < 3c^2 - 4c^3$ and $0 < c < \frac{3}{4}$.

 $\pm 0.4, y_0 = \pm 0.394388$, respectively. Similarly, the profiles of the kink-like and antikink-like solutions $\varphi(\xi)$ are given in Figures 10(a)–10(l) by taking the initial point (φ_0, y_0) with $\varphi_0 = -0.75, y_0 = \pm 0.0312059, \ \varphi_0 = -0.4, y_0 = \pm 0.159326, \ \varphi_0 = -0.1, y_0 = \pm 0.160895, \ \varphi_0 = 0.1, y_0 = \pm 0.160895, \ \varphi_0 = 0.4, y_0 = \pm 0.159326, \ \varphi_0 = -0.75, y_0 = \pm 0.0312059$, respectively.

Declarations

Conflict of interest The authors declare no conflict of interest.

References

- [1] A Constantin. On the scattering problem for the Camassa-Holm equation, Proceedings of the Royal Society A: Mathematical, Physical and Engineering Sciences, 2001, 457(2008): 953-970.
- [2] M B Hossen, H O Roshid, M Z Ali. Characteristics of the solitary waves and rogue waves with interaction phenomena in a (2+1)-dimensional breaking soliton equation, Physics Letters A, 2018, 382(19): 1268-1274.

- [3] M B Hossen, H O Roshid, M Z Ali, et al. Novel dynamical behaviors of interaction solutions of the (3+1)-dimensional generalized B-type Kadomtsev-Petviashvili model, Physica Scripta, 2021, 96(12): 125236.
- [4] R Camassa, D D Holm. An integrable shallow water equation with peaked solitons, Physical Review Letters, 1993, 71(11): 1661-1664.
- [5] V Novikov. Generalizations of the Camassa-Holm equation, Journal of Physics A: Mathematical and Theoretical, 2009, 42(34): 342002.
- [6] A N W Hone, J Wang. Integrable peakon equations with cubic nonlinearity, Journal of Physics A: Mathematical and Theoretical, 2008, 41(37): 372002.
- [7] A N W Hone, H Lundmark, J Szmigielski. Explicit multipeakon solutions of Novikov's cubically nonlinear integrable Camassa-Holm type equation, Dynamics of Partial Differential Equations, 2009, 6(3): 253-289.
- [8] K Grayshan. Peakon solutions of the Novikov equation and properties of the data-to-solution map, Journal of Mathematical Analysis and Applications, 2013, 397(2): 515-521.
- [9] X Liu, Y Liu, C Qu. Stability of peakons for the Novikov equation, Journal de Mathématiques Pures et Appliquées, 2014, 101(2): 172-187.
- [10] J Li. Exact cuspon and compactons of the Novikov equation, International Journal of Bifurcation and Chaos, 2014, 24(3): 1450037.
- [11] C Pan, S Li. Further results on the smooth and nonsmooth solitons of the novikov equation, Nonlinear Dynamics, 2016, 86(2): 779-788.
- [12] L Zhang, R Tang. Bifurcation of peakons and cuspons of the integrable Novikov equation, Proceedings of the Romanian Academy Series A: Mathematics, Physics, Technical Sciences, Information Science, 2015, 16(2): 168-175.
- [13] A G Rasin, J Schiff. A simple-looking relative of the Novikov, Hirota-Satsuma and Sawada-Kotera equations, Journal of Nonlinear Mathematical Physics, 2019, 26(4): 555-568.
- [14] M B Hossen, H O Roshid, M Z Ali. Multi-soliton, breathers, lumps and interaction solution to the (2+1)-dimensional asymmetric Nizhnik-Novikov-Veselov equation, Heliyon, 2019, 5(10): e02548.
- [15] L Zhao, S Zhou. Symbolic analysis and exact travelling wave solutions to a new modified Novikov equation, Applied Mathematics and Computation, 2010, 217(2): 590-598.
- [16] X Deng. Exact travelling wave solutions for the modified Novikov equation, Nonlinear Analysis-Modelling and Control, 2015, 20(2): 226-232.
- [17] Z Wen, L Shi. Dynamics of bounded traveling wave solutions for the modified Novikov equation, Dynamic Systems and Applications, 2018, 27(3): 581-591.

- [18] B Moon. The existence of the single peaked traveling waves to the μ -Novikov equation, Applicable Analysis, 2018, 97(9): 1540-1548.
- [19] B Moon. Single peaked traveling wave solutions to a generalized μ -Novikov Equation, Advances in Nonlinear Analysis, 2021, 10(1): 66-75.
- [20] Z Wen, H Li, Y Fu. Abundant explicit periodic wave solutions and their limit forms to space-time fractional Drinfel'd-Sokolov-Wilson equation, Mathematical Methods in the Applied Sciences, 2021, 44(8): 6406-6421.
- [21] Z Wen. The generalized bifurcation method for deriving exact solutions of nonlinear spacetime fractional partial differential equations, Applied Mathematics and Computation, 2020, 366: 124735.
- [22] Z Wen. Bifurcations and exact traveling wave solutions of a new two-component system, Nonlinear Dynamics, 2017, 87(3): 1917-1922.
- [23] Z Wen. Bifurcations and exact traveling wave solutions of the celebrated Green-Naghdi equations, International Journal of Bifurcation and Chaos, 2017, 27(7): 1750114.
- [24] C Pan, Y Yi. Some extensions on the soliton solutions for the Novikov equation with cubic nonlinearity, Journal of Nonlinear Mathematical Physics, 2015, 22(2): 308-320.
- [25] L Shi, Z Wen. Dynamics of traveling wave solutions to a highly nonlinear Fujimoto-Watanabe equation, Chinese Physics B, 2019, 28(4): 040201.
- [26] L Shi, Z Wen. Several types of periodic wave solutions and their relations of a Fujimoto–Watanabe equation, Journal of Applied Analysis and Computation, 2019, 9(4): 1193-1203.
- [27] M Wei. Bifurcations of traveling wave solutions for a modified Novikov's cubic equation, Qualitative Theory of Dynamical Systems, 2019, 18(2): 667-686.
- [28] Z Wen. Qualitative study of effects of vorticity on traveling wave solutions to the two-component Zakharov-Itō system, Applicable Analysis, 2021, 100(11): 2334-2346.
- [29] Z Zhang, T Ding, W Huang, et al. Qualitative theory of differential equations, American Mathematical Society, Providence, 1992.
- [30] Z S Wen, L J Shi. Dynamical behaviors of traveling wave solutions to a Fujimoto-Watanabe equation, Chinese Physics B, 2018, 27(9): 090201.

¹School of Sciences, Xichang University, Xichang 615000, China.

²School of Mathematical Sciences, Huaqiao University, Quanzhou 362021, China.

³School of Mathematics and Statistics, Shaoguan University, Shaoguan 512005, China. Email: wenzhenshu@hqu.edu.cn